A hypoxic microfluidic organoid-on-a-chip system for studying the efficacy of metronidazole-modified nanomaterials against cholangiocarcinoma established within the chip

Ao Xie, [ab] Zipeng Yao, [abf] Qijun Du, [ab] Mengjia Xia, [f] Qinrui Lu, [ab] Jiashu Wang, [ab] Wenqi Hu, [ab] Lin Wu, [ab] Chenwei Sun, [ab] Youlong Yang, [ab] Di Wu, [de] Haijie Hu, [g] Guohua Wu*[c] and Shuqi Wang*[abfh]

a. College of Biomedical Engineering, Sichuan University, Chengdu 610065, China.

b. National Engineering Research Center for Biomaterials, Sichuan University, Chengdu 610065, China.

c. Luoyang Key Laboratory of Clinical Multiomics and Translational Medicine, Henan Key Laboratory of Rare Diseases, Endocrinology and Metabolism Center, The First Affiliated Hospital, and College of Clinical Medicine of Henan University of Science and Technology, Luoyang 471003, China.

d. Department of Respiratory and Critical Care Medicine, West China Hospital, Sichuan University, Chengdu 610045, China.

e. State Key Laboratory of Respiratory Health and Multimorbidity, West China Hospital, Sichuan University, Chengdu 610045, China.

f. Tianfu Jincheng Laboratory, City of Future Medicine, Chengdu 641400, China.

g. Division of Biliary Surgery, Department of General Surgery, West China Hospital, Sichuan University, Chengdu 610041, China.

h. Clinical Research Center for Respiratory Disease, West China Hospital, Sichuan University, Chengdu 610045, China.

Corresponding authors:

Shuqi Wang: shuqi@scu.edu.cn

Guohua Wu: wuguohua@zju.edu.cn

a b

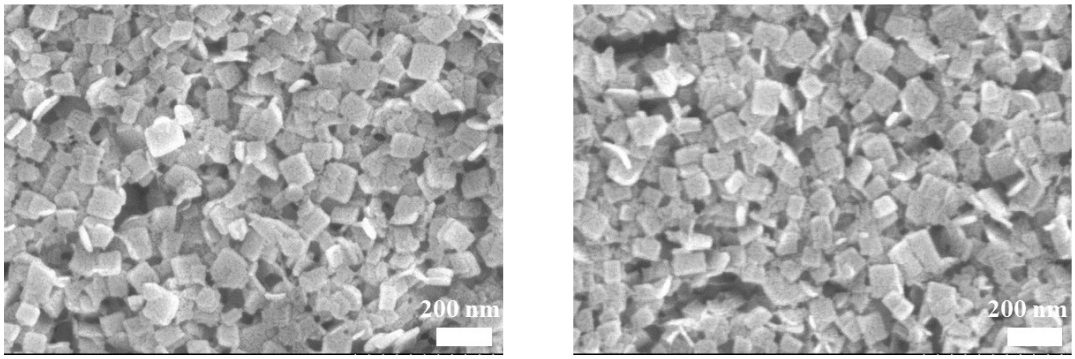

Fig. S1 The SEM image of BMMN (a) and BMMNP NPs (b). Scale bar: 200 µm.

a

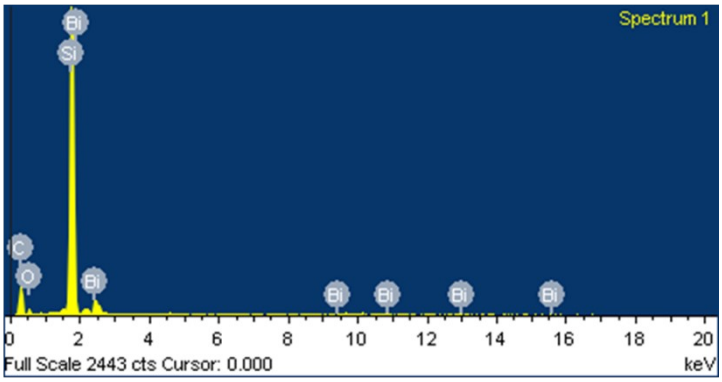

b

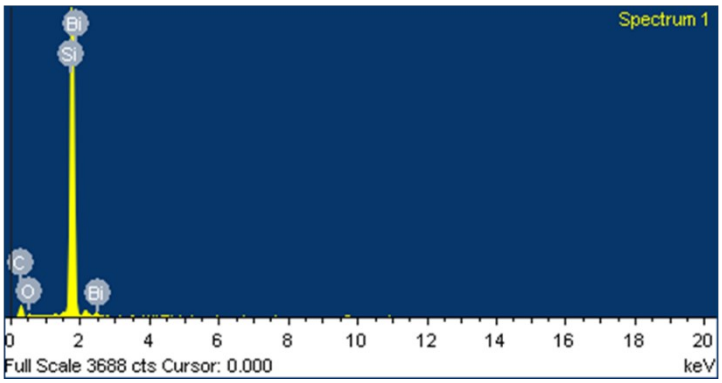

Fig. S2 The EDS of BMMN (a) and BMMNP NPs (b).

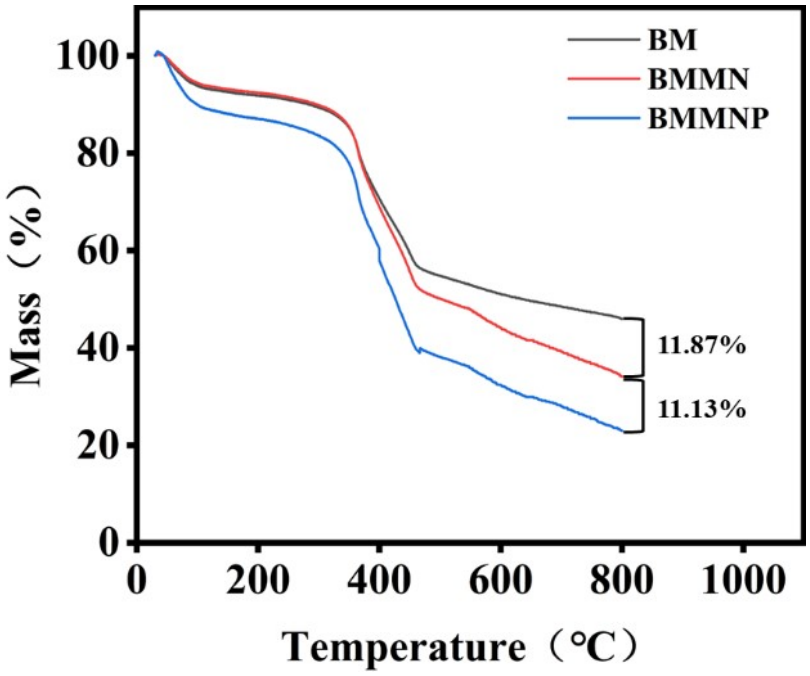

Fig. S3 The TGA curves of BM, BMMN and BMMNP NPs.

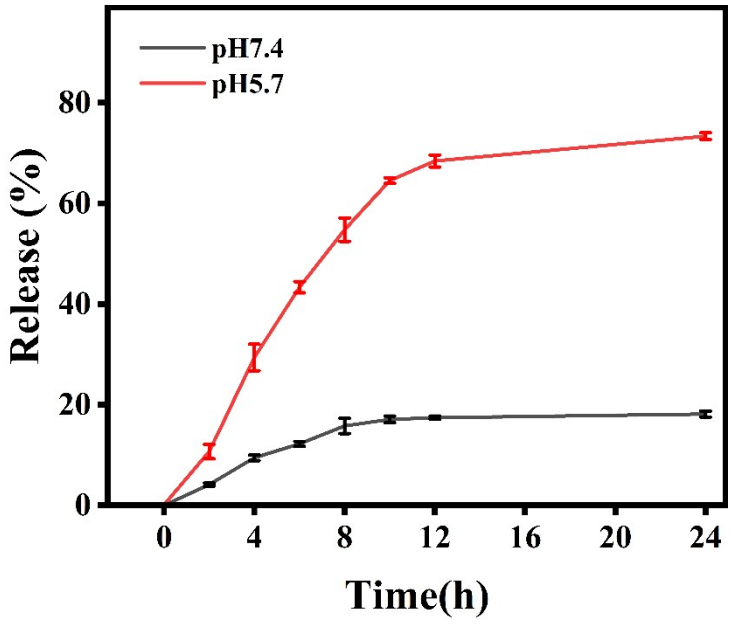

Fig. S4 *In vitro* drug release profile of MN from BM-MN@PDA NPs in neutral and weakly acidic PBS (n = 3).

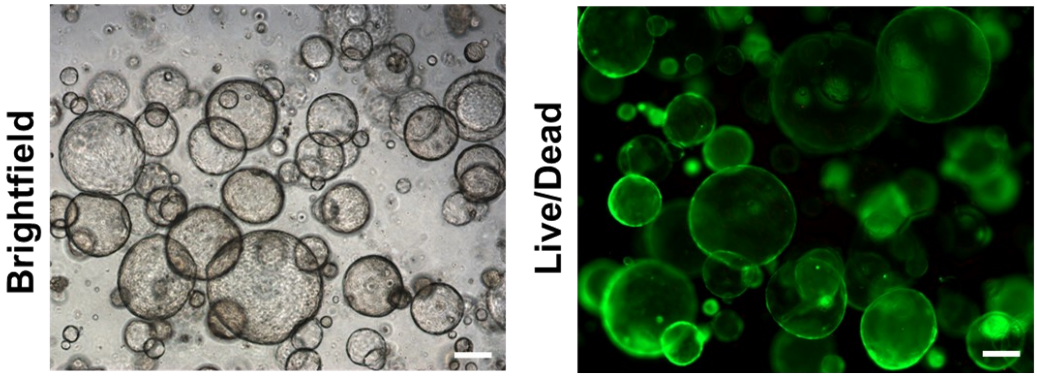

Fig. S5 Viability assessment of patient-derived (CCOs). Bright-field (left) and Live/Dead staining (right) Scale bar: 200 μm.

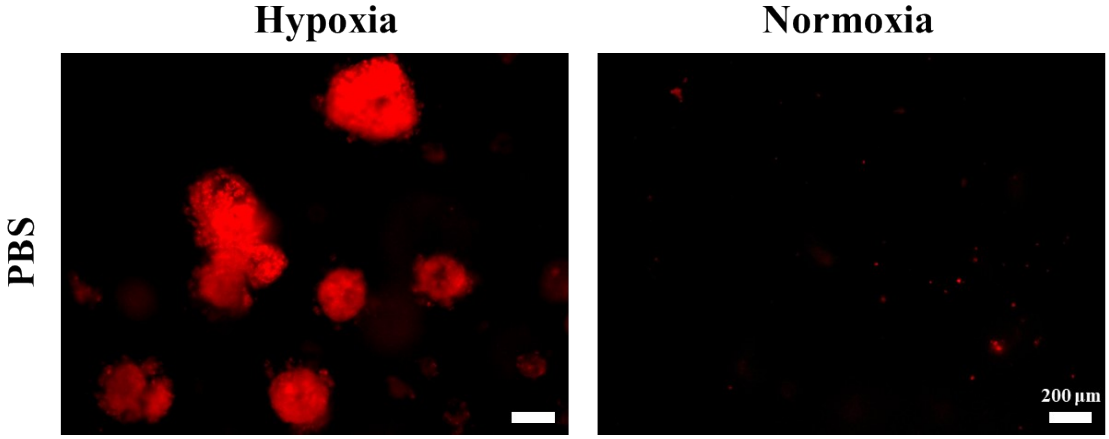

Fig. S6 Fluorescence images of hypoxia markers (Ru(ddp)) in organoid from normoxic and hypoxic microfluidic chips. Scale bar: 200 μm.

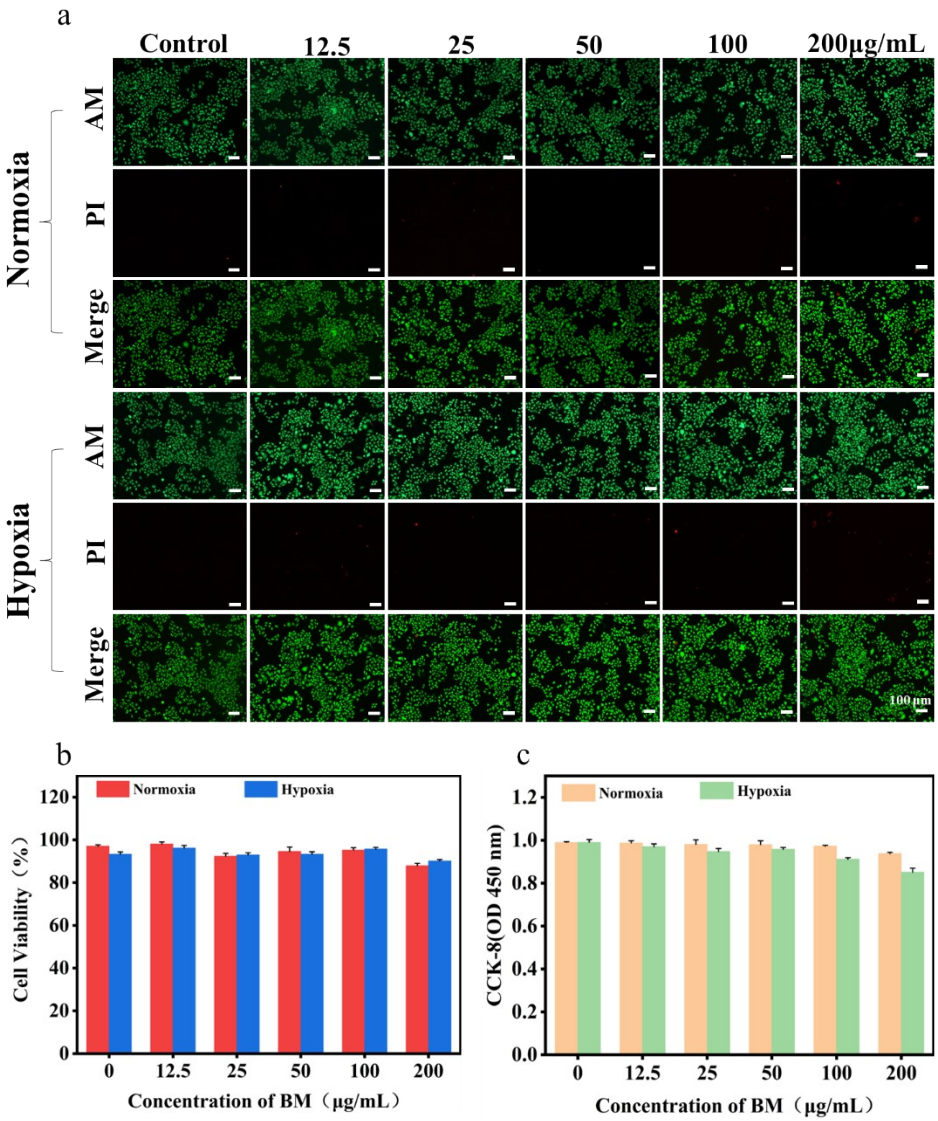

Fig. S7 (a) Under normoxic and hypoxic conditions, AM/PI staining used for evaluating the BM NPs cytotoxicity on HepG2 cells. Scale bar: 100 μm. (b) Cell Viability of HepG2 after BM NPs treatments (n = 3). (c) CCK-8 results after BM NPs treatments (n = 3).

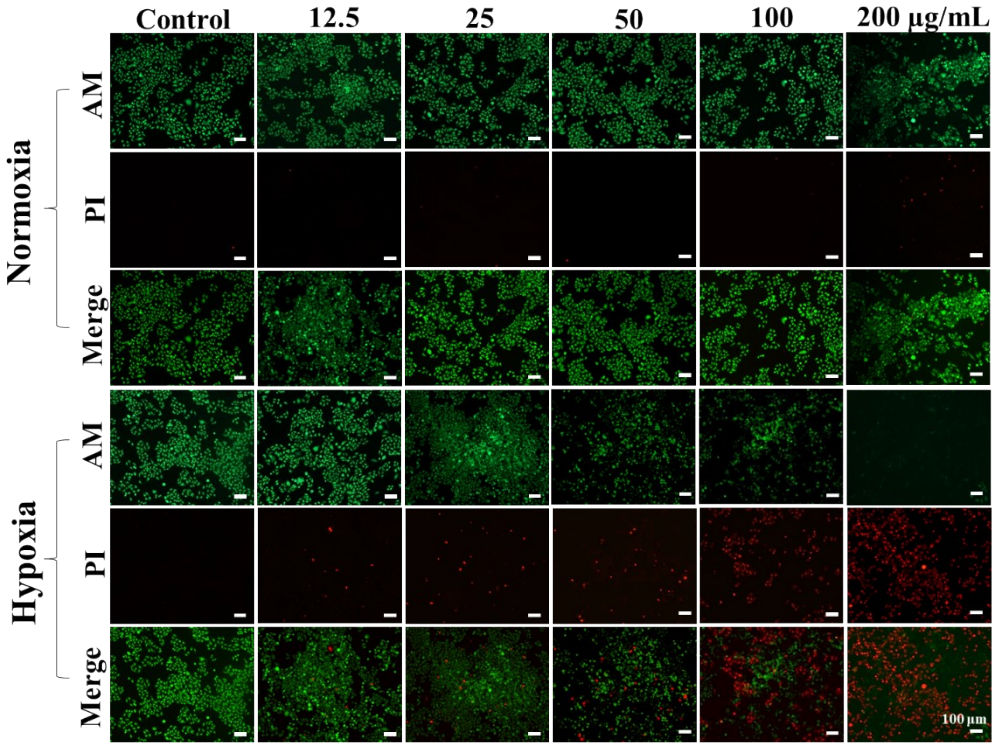

Fig. S8 Under normoxic and hypoxic conditions, the concentration of BMMNP NPs (0-200μg/ml) respectively affects the cytotoxicity to HepG2 cells. Scale bar: 100 μm.

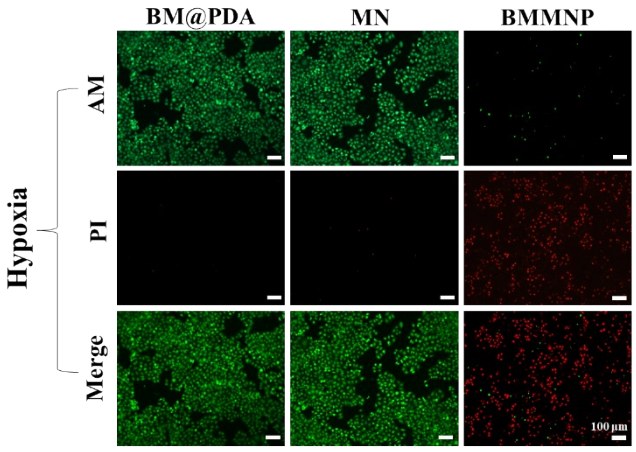

Fig. S9 Fluorescence images of Live/Dead staining assay during drug exposure under hypoxic conditions. Scale bar:100 μm.

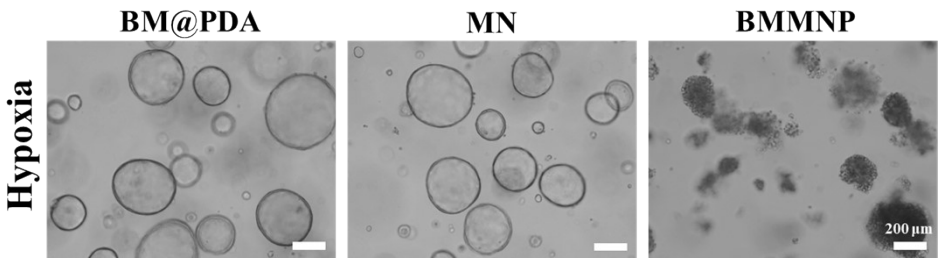

Fig. S10 Bright-field images of CCOs treated with BM@PDA, Free MN, and BMMNP under hypoxic conditions. Scale bar: 200 μm.

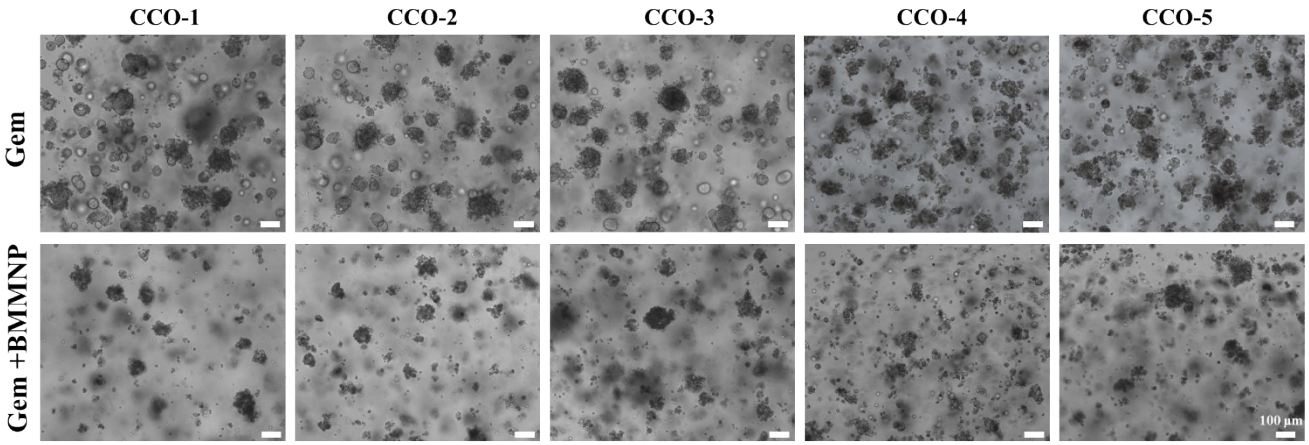

Fig. S11 Bright-field images showing the morphological response of CCOs derived from five different patients following drug treatment. Scale bar: 100 μm.